Axion detection by Rydeberg atoms

Zhiguang Xiao,
Nuclear & particle group in Si Chuan University
Axion 2023@Xi'an， 2023.07.25

四川大學
SICHUAN UNIVERSITY

Collaboration institute:
Technology and engineering center for space utilization, Chinese academy of science

中国科学院空间应用工程与技术中心
Technology and Engineering Center for Space Utilization, Chinese Academy of Sciences

Contents

1

Background

Strong CP -- axion

- CP breaking term in QCD

$$\mathcal{L}_\theta = -\frac{\bar{\theta}\alpha_s}{8\pi} G^{\mu\nu a}\tilde{G}^a_{\mu\nu}$$

- Induce a Neutron Electric Dipole Moment (nEDM)

$$\mathcal{L}_{dn} = -\frac{i}{2} d_n \bar{\Psi}_N \sigma_{\mu\nu}\gamma_5 \Psi_N F^{\mu\nu}, \;\; d_n = C_{EDM} e\bar{\theta}; \quad C_{EDM} = 2.4(1.0)\times 10^{-16}\mathrm{cm}$$

[M. Pospelov and A. Ritz,NPB573,177]

- Experimental upper bound:

$$|d_n| < 1.8\times 10^{-26}\, e\,\mathrm{cm}, \quad \Rightarrow |\bar{\theta}| \lesssim 10^{-10}$$

.[C. A. Baker et al., PRL97, 131801 (2006);
C. Abel et al.(nEDM), PRL124,8,081803 (2020)]

- Why is it so small? The Strong CP problem.

Strong CP -- axion solution

[R. D. Peccei and H. R. Quinn,PRL38(1977),1440;PRD16,1791]

1. Assume a $U(1)_{PQ}$ axial symmetry: anomalously coupled to gluon

2. Spontaneously broken.

3. The would-be Nambu-Goldstone boson: Axion a

4. Couple to the gluon:

$$L_{aG} = \left(\frac{a}{f_a} - \theta\right)\frac{\alpha_s}{8\pi} G^{\mu\nu a}\tilde{G}^a_{\mu\nu}$$

5. Minimum of the effective potential dynamically generates

$$\bar{\theta} = \frac{\langle a \rangle}{f_a} - \theta = 0$$

Vafa, V., and E. Witten, 1984, PRL53, 535.

Strong CP -- axion: theoretical models

- Original PQWW: (Weinberg，(1978)； Wilczek (1978)

  PQ breaking scale f_a~ EW breaking scale

  Ruled out by stellar evolution constraints

  $f_a > 10^9$ GeV

- Invisible axion models: PQ breaking at much higer energy scale
  - KSVZ: (Kim1979;Shifman,Vainshtein,Zakharov 1980)
  - DFSZ:(Dine,Fishler,Srednicki,1981;Zhitnitsky(1980))

- Axion mass: very small

$$m_a = 5.691(51)(\frac{10^9 GeV}{f_a})\ \mathrm{meV}$$

(PDG2022; Gorghetto, Villadoro,JHEP 03,033(2019))

$f_a \sim 10^{10}$--10^{13}GeV, $m_a \sim$ 1μeV--100μeV

Axion Couplings:

- Couplings: suppressed by f_a , very small

- Various couplings: (PDG 2022)

$$\mathcal{L}_{aN\gamma} = -\frac{i}{2} g_{aN\gamma}\, a\, \overline{\Psi}_N \sigma_{\mu\nu}\gamma_5 \Psi_N F^{\mu\nu} , \qquad g_{an\gamma} = -g_{ap\gamma} = e\,\frac{C_{\mathrm{EDM}}}{f_a} = (3.7 \pm 1.5) \times 10^{-3} \left(\frac{1}{f_a}\right) \frac{1}{\mathrm{GeV}} .$$

$$\mathcal{L}_{aff} = \frac{C_f}{2 f_a}\, \partial_\mu a\, \bar{\Psi}_f \gamma^\mu \gamma_5 \Psi_f$$

$$C_e \simeq \frac{3\alpha^2}{4\pi^2}\left[\frac{E}{N}\log\left(\frac{f_a}{m_e}\right) - 1.92\log\left(\frac{\Lambda_\chi}{m_e}\right)\right] \quad , \quad \ldots\ldots$$

[hadronic axion model,M. Srednicki, NPB260, 689 (1985)]
[S. Chang and K. Choi, Phys. Lett. B316, 51 (1993)]

$$\mathcal{L}_{a\gamma\gamma} = -\frac{g_{a\gamma\gamma}}{4}\, a\, F_{\mu\nu}\tilde{F}^{\mu\nu} = g_{a\gamma\gamma}\, a\, \mathbf{E}\cdot\mathbf{B} ,$$

$$g_{a\gamma\gamma} = \frac{\alpha}{2\pi f_a}\left(\frac{E}{N} - 1.92(4)\right) = \left(0.203(3)\frac{E}{N} - 0.39(1)\right)\frac{m_a}{\mathrm{GeV}^2}$$

[G. Grilli di Cortona et al., JHEP 01, 034 (2016)]

Coupling to E-M fields:

$$\mathcal{L}_{a\gamma\gamma} = -\frac{g_{a\gamma\gamma}}{4}\, a\, F_{\mu\nu}\tilde{F}^{\mu\nu} = g_{a\gamma\gamma}\, a\, \mathbf{E}\cdot\mathbf{B}\,,$$

$$g_{a\gamma\gamma} = \frac{\alpha}{2\pi f_a}\left(\frac{E}{N} - 1.92(4)\right) = \left(0.203(3)\frac{E}{N} - 0.39(1)\right)\frac{m_a}{\mathrm{GeV}^2}$$

Benchmark:

- DFSZ : E/N=8/3
- KSVZ : E/N=0

Much weaker than E-M interaction:

$f_a > 10^9$ GeV, 10 orders of magnitude weaker.

Axion to photon conversion

Axion-E-M field coupling provides a source in the Maxwell's Eq

$$\nabla \cdot \vec{E} = g_{a\gamma\gamma} \vec{B} \cdot \nabla a,$$

$$\nabla \times \vec{B} - \frac{\partial \vec{E}}{\partial t} = g_{a\gamma\gamma} \left[\vec{E} \times \nabla a - \vec{B} \frac{\partial a}{\partial t} \right],$$

$$\Box a = g_{a\gamma\gamma} \vec{E} \cdot \vec{B} - m_a^2 a$$

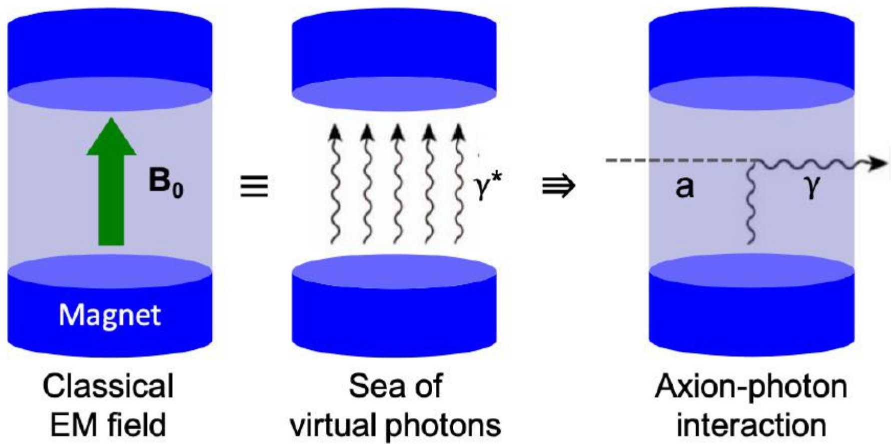

Galactic halo: ultralight Axion field can be treated classcally

$$a(x, t) = a_0 \cos(\omega_a t + \phi_a), \quad \hbar\omega_a \simeq m_a c^2 + \frac{1}{2} m_a v^2$$

(Figure from Y.K. Semertzidis, S.W.Youn, Sci.Adv.8,eabm9928(2022))

Strong magnetic field can stimulate the conversion of axion to photons.

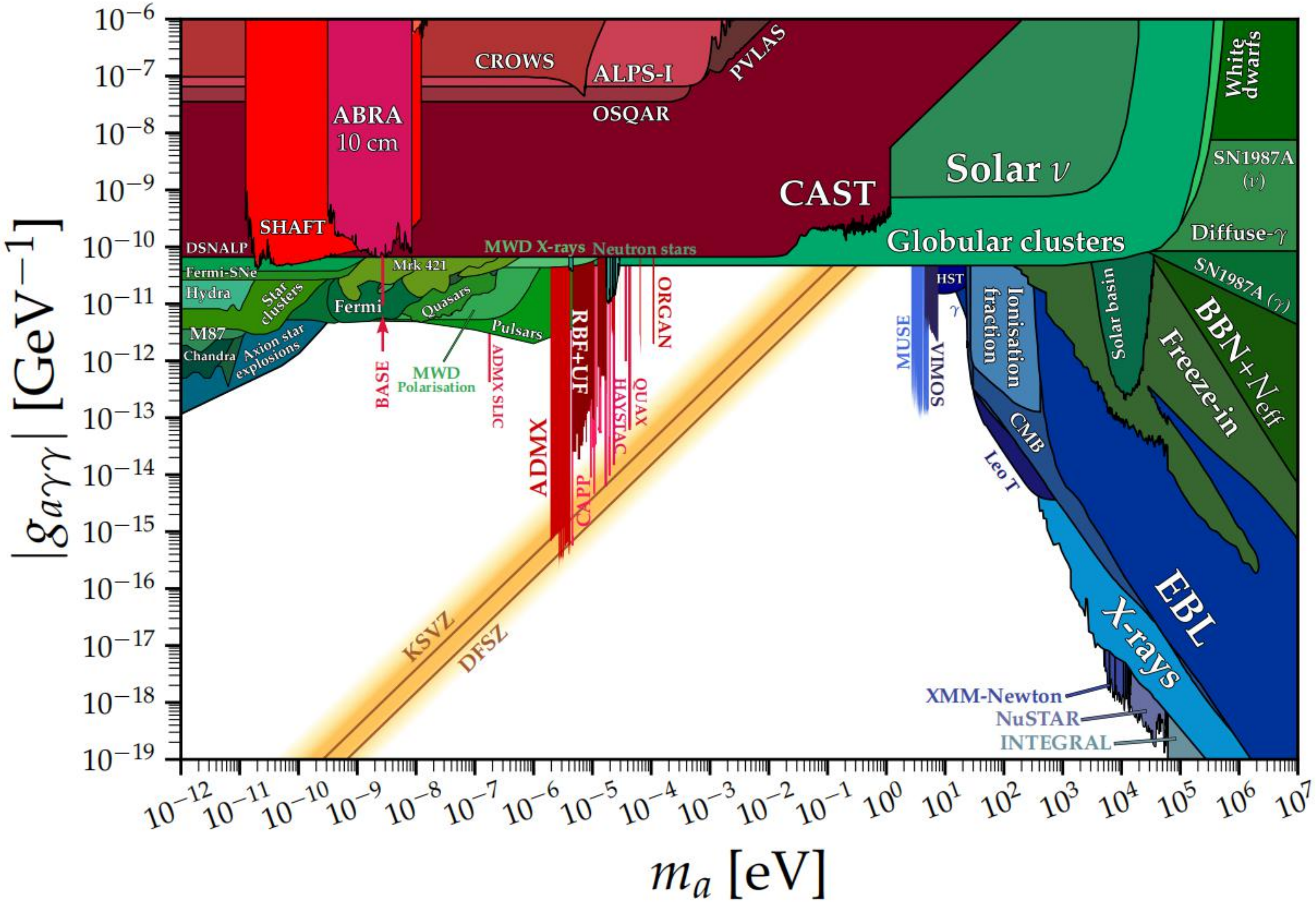

Exclusion plot for a-γ-γ coupling. Figure courtesy of Ciaran O’ Hare

[“cajohare/axionlimits: Axionlimits” ,2021,https://cajohare.github.io/AxionLimits/].

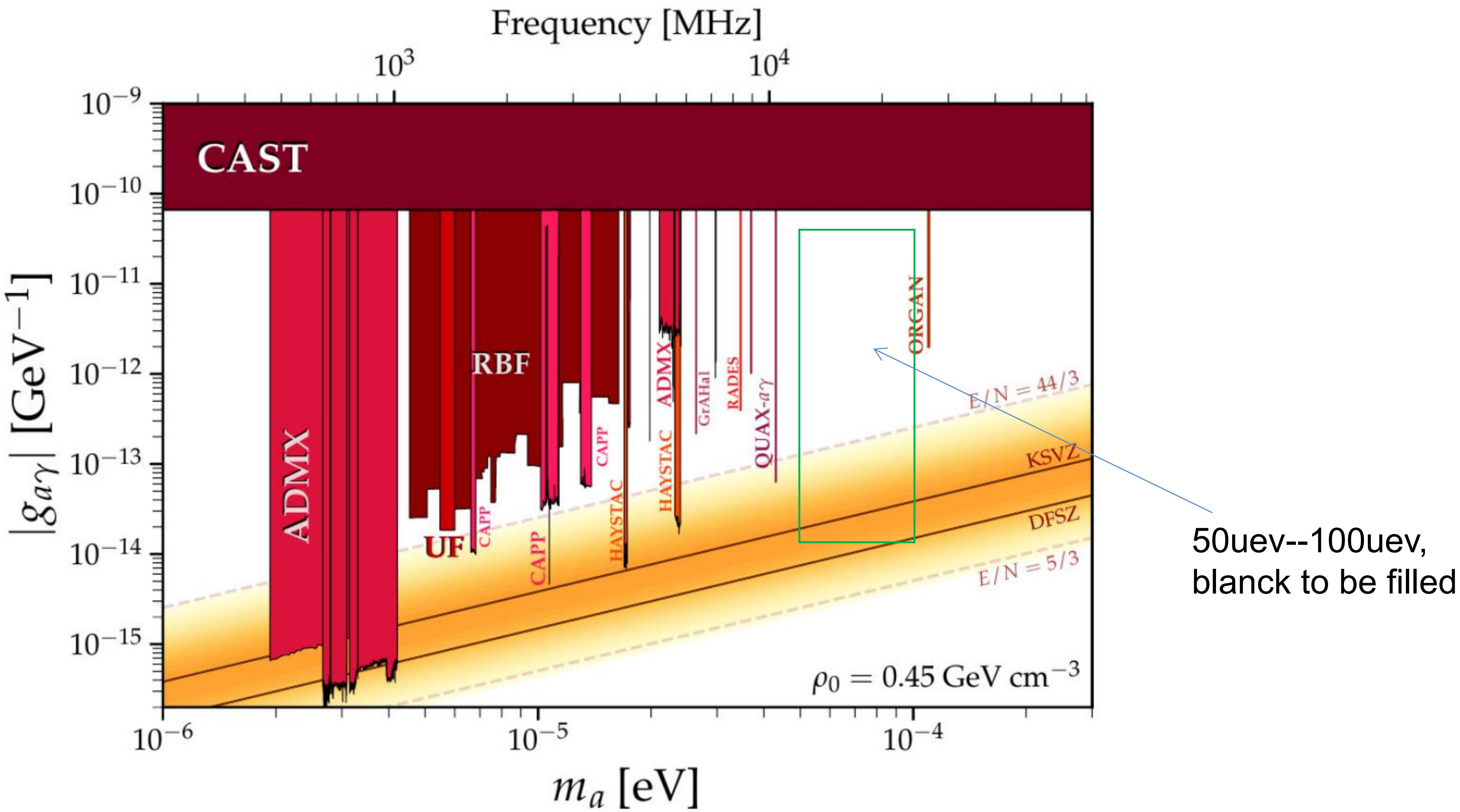

Exclusion plot for a-γ-γ coupling on the parameter space of microwave cavity experiments. Figure courtesy of Ciaran O′ Hare

[“cajohare/axionlimits: Axionlimits” ,2021,https://cajohare.github.io/AxionLimits/].

Haloscope: (Sikivie PRL51(1983))

- Galactic halo model: The dark matter clusters around the galaxy and form a halo. (Gates et al., Astrophys.J.449(1995)，123)

$$\rho_{dm} = 0.450 GeV/cm^3 \sim 10^{-24} g/cm^3$$

- If we choose $m_a = 1\mu eV$--$100\mu eV$, $f_a \sim 10^{10}$-10^{13}GeV,

  Axion number density 10^{12} -- 10^{15} /cm^3

- Photon generation: microwave region,

  f ~ 100MHz--100GHz, Wave length ~ 0.1cm-- 1meter

Haloscope:

- Rate of photon generation: a GUT model, $g_{a\gamma\gamma} = \frac{e^2 N}{3\pi^2 v}$ (Sikivie PRL51(1983), PRD32,2988)

$$\frac{\text{No. of photons}}{\text{time}} \simeq \frac{1.6}{10^6 \text{ sec}} \frac{V}{1 \text{ cm}^3} \left(\frac{B_0}{1\text{T}}\right)^2 R(m_a) \left(\frac{N}{6r}\right)^2$$

A rough estimate: for $R(m_a)$~10, V~ (30 cm)^3, B_0~ 10T, there are about 45 $a \to \gamma$ transitions per second ~10^{-24}W for μeV axion. (Sikivie PRL51(1983))

- Cavity haloscope: In resonant Cavity, microwave power

$$P_a = \left(\frac{\alpha_{\text{em}} c_{a\gamma\gamma}}{2\pi F_a}\right)^2 V B_0^2 \rho_a C_{lmn} \frac{1}{m_a} \min(Q_L, Q_a)$$

$$= 0.5 \times 10^{-26} \text{ W} \left(\frac{V}{500\ell}\right) \left(\frac{B_0}{7\text{T}}\right)^2 C_{lmn} \left(\frac{c_{a\gamma\gamma}}{0.72}\right)^2$$

$$\times \left(\frac{\rho_a}{0.5 \times 10^{-24} \text{ g cm}^{-3}}\right)$$

$$\times \left(\frac{m_a}{2\pi(\text{GHz})}\right) \min(Q_L, Q_a),$$

Sikivie 1985 ; PRD32,2988; Kim RMP 82, 557

$$C_{lmn} = \frac{\left| \int_V d^3x \vec{E}_\omega \cdot \vec{B}_0 \right|^2}{B_0^2 V \int_V d^3x \epsilon |\vec{E}_\omega|^2}$$

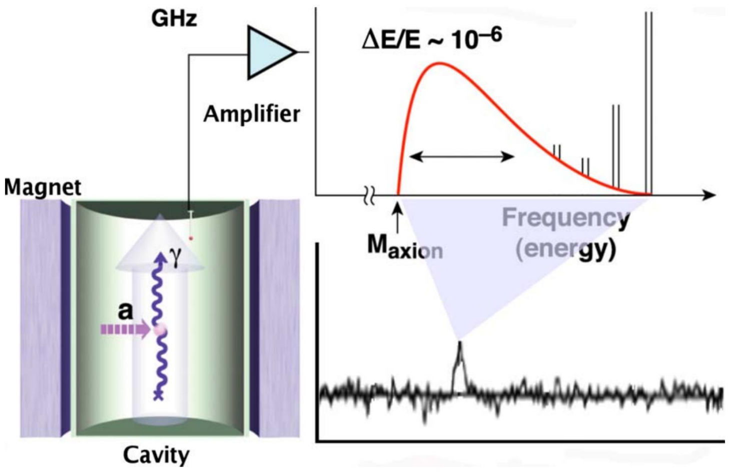

From Kim,et al. Rev.Mod.Phys,82,557

Detection methods

ADMX

- Cavity haloscope:
  Suitable for < 50 ueV (12 GHz).

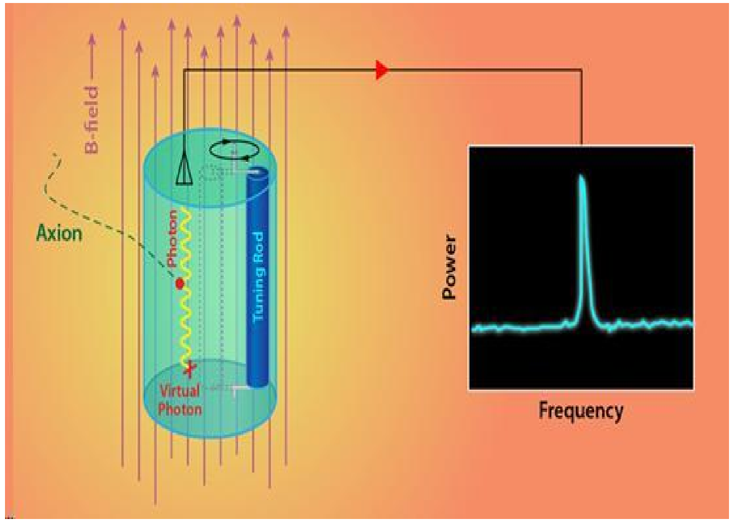

Higher mass problems:
1. Need smaller cavity. lower sensitivity.
2. The resonator quality factor decreases at high frequency.
3. Noise of the amplifier increases with frequency: Both for HEMT and SQUIDs (Lamoreaux, et al., PRD88(2013)035020)

Running:

- ADMX(Washington University):
  - 2.66-3.31 ueV
  - 17.38-17.57 ueV
  - 21.03-23.98 ueV
  - 29.67-29.79 ueV
- HAYSTAC(Yale University):
  - 23.15-24 ueV,
- QUAX-ay(Italy) :
  - 43.0145-43.0219 ueV
- CAPP(Korea):
  - 10.7162-10.7186 ueV
- TASEH(Taiwan, China):
  - 19.4687-19.8436 ueV

Under construction:

- ORGAN(Australia) :
  - 109.835-109.840ueV
- MadMax(Germany):
  - 40-400 ueV

2

Microwave detection with Rydberg atoms

What is the Rydberg atoms?

$$E_{nl} = -\frac{R_A hcZ^{*2}}{n^2} = -\frac{R_A hc}{(n-\Delta_l)^2}$$

$$\delta_{n\ell j} = \delta_0 + \frac{\delta_2}{(n-\delta_0)^2} + \frac{\delta_4}{(n-\delta_0)^4} + \frac{\delta_6}{(n-\delta_0)^6} + \frac{\delta_8}{(n-\delta_0)^8}, \cdots$$

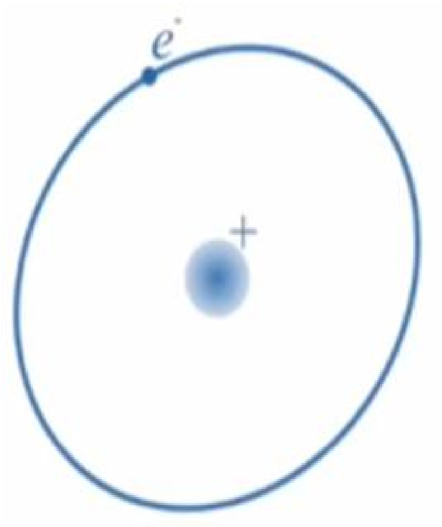

Principal quantum number: n≥10

Series		δ_0	δ_2	δ_4	δ_6	δ_8
^{7}Li	$ns_{1/2}$	0.399468	0.030233	−0.0028	0.0115	
	$np_{1/2,3/2}$	0.47263	−0.02613	0.0221	−0.0683	
	$nd_{3/2,5/2}$	0.002129	−0.01491	0.1759	−0.8507	
	$nf_{5/2,7/2}$ [b]	0.0003055(40)	−0.00126(5)			
^{23}Na	$ns_{1/2}$ [c]	1.3479692(4)	0.06137(10)			
	$np_{1/2}$ [c]	0.855424(6)	0.1222(2)			
	$np_{3/2}$ [c]	0.854608	0.1220(2)			
	$nd_{3/2,5/2}$	0.015543	−0.08535	0.7958	−4.0513	
	$nf_{5/2,7/2}$ [d]	0.001663(60)	−0.0098(3)			
^{39}K	$ns_{1/2}$	2.180197(15)	0.136(3)	0.0759	0.117	−0.206
	$np_{1/2}$	1.713892(30)	0.2332(50)	0.16137	0.5345	−0.234
	$np_{3/2}$	1.710848(30)	0.2354(60)	0.11551	1.105	−2.0356
	$nd_{3/2}$	0.276970(6)	−1.0249(10)	−0.709174	11.839	−26.689
	$nd_{5/2}$	0.277158(6)	−1.0256(20)	−0.59201	10.0053	−19.0244
	$nf_{5/2,7/2}$	0.010098	−0.100224	1.56334	−12.6851	
^{85}Rb	$ns_{1/2}$	3.13109(2)	0.204(8)	−1.8		
	$np_{1/2}$	2.65456(15)	0.388(60)	−7.904	116.437	−405.907
	$np_{3/2}$	2.64145(20)	0.33(18)	−0.97495	14,6001	−44,7265
	$nd_{3/2,5/2}$	1.347157(80)	−0.59553	−1.50517	−2.4206	19.736
	$nf_{5/2,7/2}$	0.016312	−0.064007	−0.36005	3.2390	
^{133}Cs	$ns_{1/2}$ [e]	4.049325(15)	0.246(5)			
	$np_{1/2}$ [e]	3.591556(30)	0.3714(40)			
	$np_{3/2}$ [e]	3.559058(30)	0.374(40)			
	$nd_{3/2}$ [e]	2.475365(20)	0.5554(60)			
	$nd_{5/2}$ [e]	2.466210(15)	0.0167(5)			
	$nf_{5/2}$ [e]	0.033392(50)	−0.191(30)			
	$nf_{7/2}$ [e]	0.033537(28)	−0.191(20)			

The advantages of Rydberg atoms in detecting MW

- The energy level transition dipole moment is large, easy to couple with microwave.
- Long life time: $\tau_n \propto \tilde{n}^3$, stay excited for a long time
- Measurement covers the frequency range of 1GHz-100 GHz.
  Covers the range of axion detection.
- Rydberg atoms convert microwave signals into spectral signals: high sensitivity
- The senstivity does not decrease with higher frequency.

Rydberg atoms	scale	Cs(50D)	Measurement correlation property
Energy Level	n^{-3}	6.32GHz	wide frequency range
Dipole moment	n^7	$1550ea_0$	coherent coupling easily
Atomic radius	n^2	2.3 um	Sensitive to weak field
Lifetime	n^3	78 us	Long coherence time

CARRACK Experiment in Japan

-- An experiment using Rydberg atomic in axion detection

1998-2016

[Tada et al.,PLA349 (2006) 488]

- detection method:

[conversion cavity] [detection cavity]

$$\langle \text{axions} \rangle \overset{B_0}{\underset{g_{a\gamma\gamma}}{\Longleftrightarrow}} \langle \text{photons} \rangle \overset{d}{\underset{\Omega_N}{\Longleftrightarrow}} \langle \text{atoms} \rangle$$

— $|e\rangle \rightarrow$ *selective field ionization*

$\updownarrow$

— $|g\rangle$

$\uparrow$ *laser excitation*

ground state (Rb)

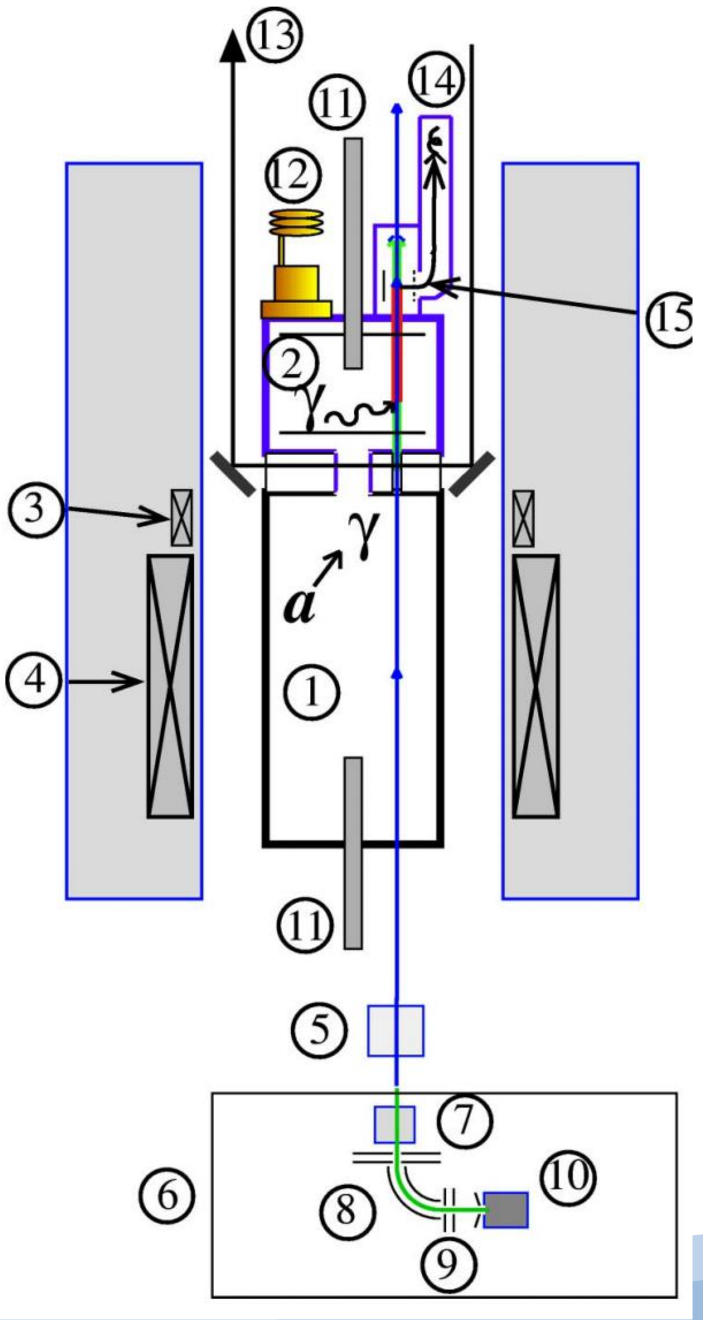

- Conversion cavity①: Axion → photon in B_0.
- Detection cavity②: separate from conversion cavity. No B_0
- Rydberg atom Rb beam at ground state goes through the conversion cavity with no effect
- In the detection cavity, the Rb are excited to |*g*> state,

  $|g\rangle+\gamma\rightarrow |e\rangle$, $E_g-E_e=E_\gamma$
- Count the excited |*e*>: selectively ionize the |*e*> state, electrons enter 14 for detection.

Japan CARRACK II Experiment

- DM center in Kyoto Univ. was closed in 2016.
- CARRACK was moved to Osaka Univ.
- 2017~ Project in Research center for Nuclear Physics

"Search for Axion to Resolve the Strong-CP and Dark Matter Problem"

Target mass: $\sim 10\ \mu eV \rightarrow \sim 100\ \mu eV$

The Rydberg-Atom-Cavity Axion Search

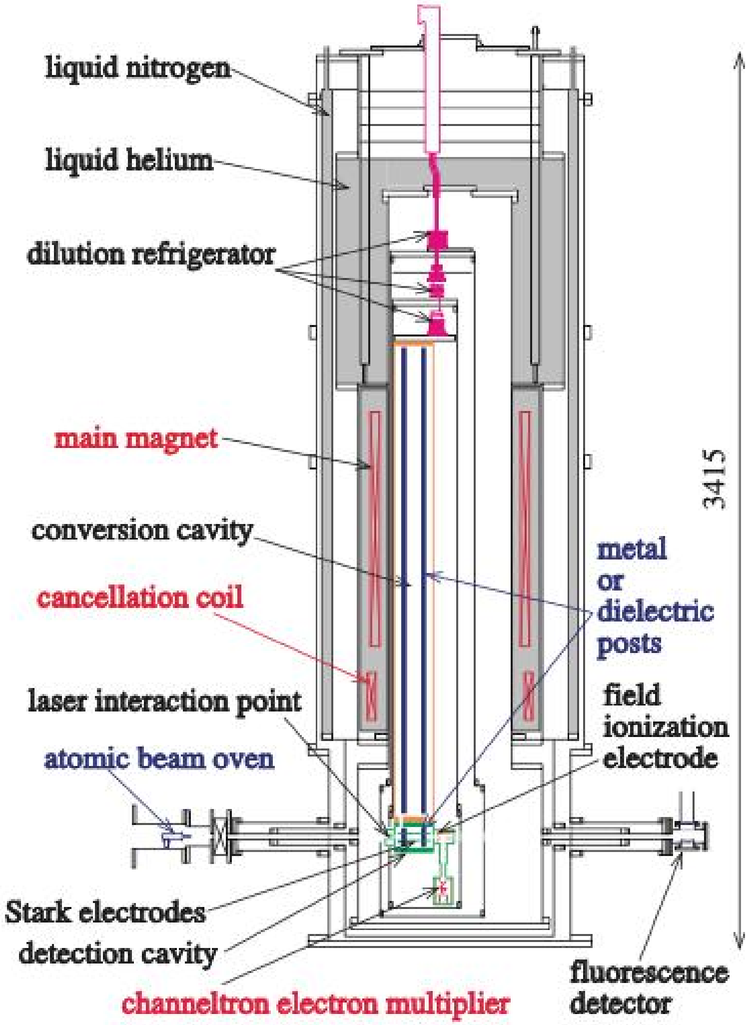

[Tada et al., NPB71,164]

Fig. 1. The layout of CARRACK II.

Microwave detection using EIT-AT effect

New quantum precision measurement technology
Using EIT-AT splitting [Nat.Phys.8(2012),819]

- EIT: Electromagnetic induced transparency.
  (Alzetta,et al., NuoCim,B36,5(1976);Whitley,Stroud,TRA14,11498)
  AT: Autler-Townes splitting. (AC stark eff)
  (Autler, Townes,PR100,703(1955))
- Converts microwave signals into spectral signals

EIT:

- Strong Coupling laser + Weak Probe laser
- The gas become transparent to the probe laser, when $E_{32}=h\nu_c$, $E_{21}=h\nu_p$

AT:

- A weak MW resonant with E_{34} causes energy spliting of E_3.
- When the coupling laser scans the frequency, we see two transmission maxima.
- Δf proportional to the electric field strength of the MW

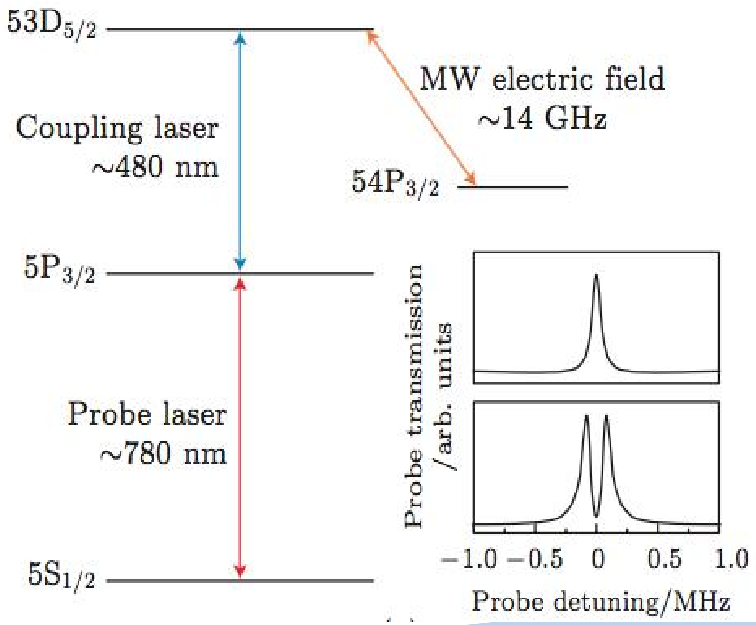

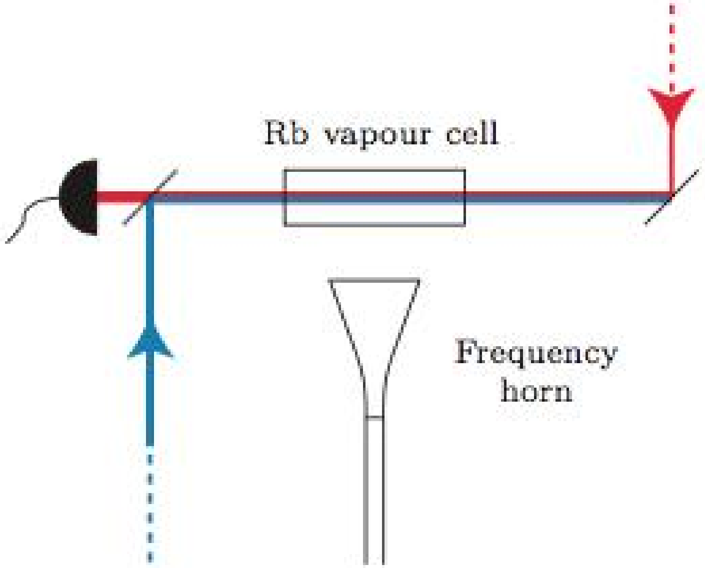

Rydberg atomic microwave detection

□The limit sensitivity:

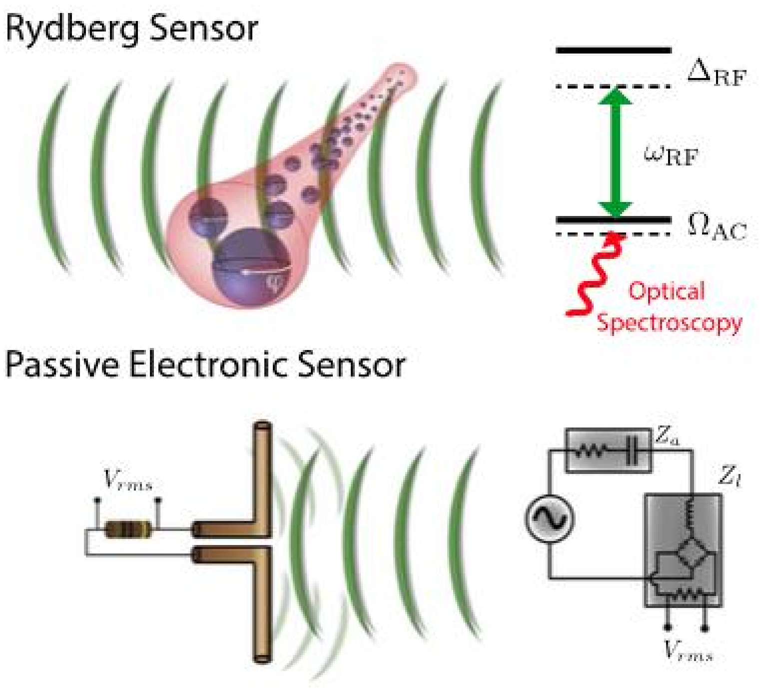

$$|E| = \frac{\hbar}{\wp_{MW}}\Omega_{RF} = \frac{\hbar}{\wp_{MW}} 2\pi \frac{\lambda_P}{\lambda_C}\Delta f$$

Shot noise limit： -220 dBm/Hz

Still could be reduced

$$I_A = \frac{-E_{0\theta}\cdot l}{\pi(Z_0 + Z_A)\sin(kl)} f(\theta,\varphi)$$

Thermal noise limit： −174 dBm/Hz

Room temperature

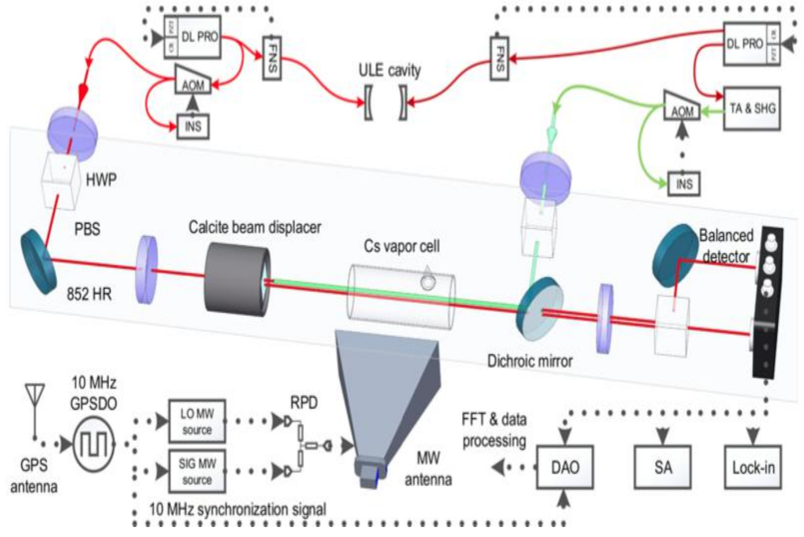

Nat Phys, 16 (2020) 911

Sensitivity： -180dBm/Hz

$g_{a\gamma\gamma}$~ 100 --- 1000$g_{a\gamma\gamma}$ (DSFZ,KSVZ)
Still has much improvement potential

Axion photon： sensitivity requirement ~ -230dBm/Hz

3

Detection Proposal

Conceptual Design

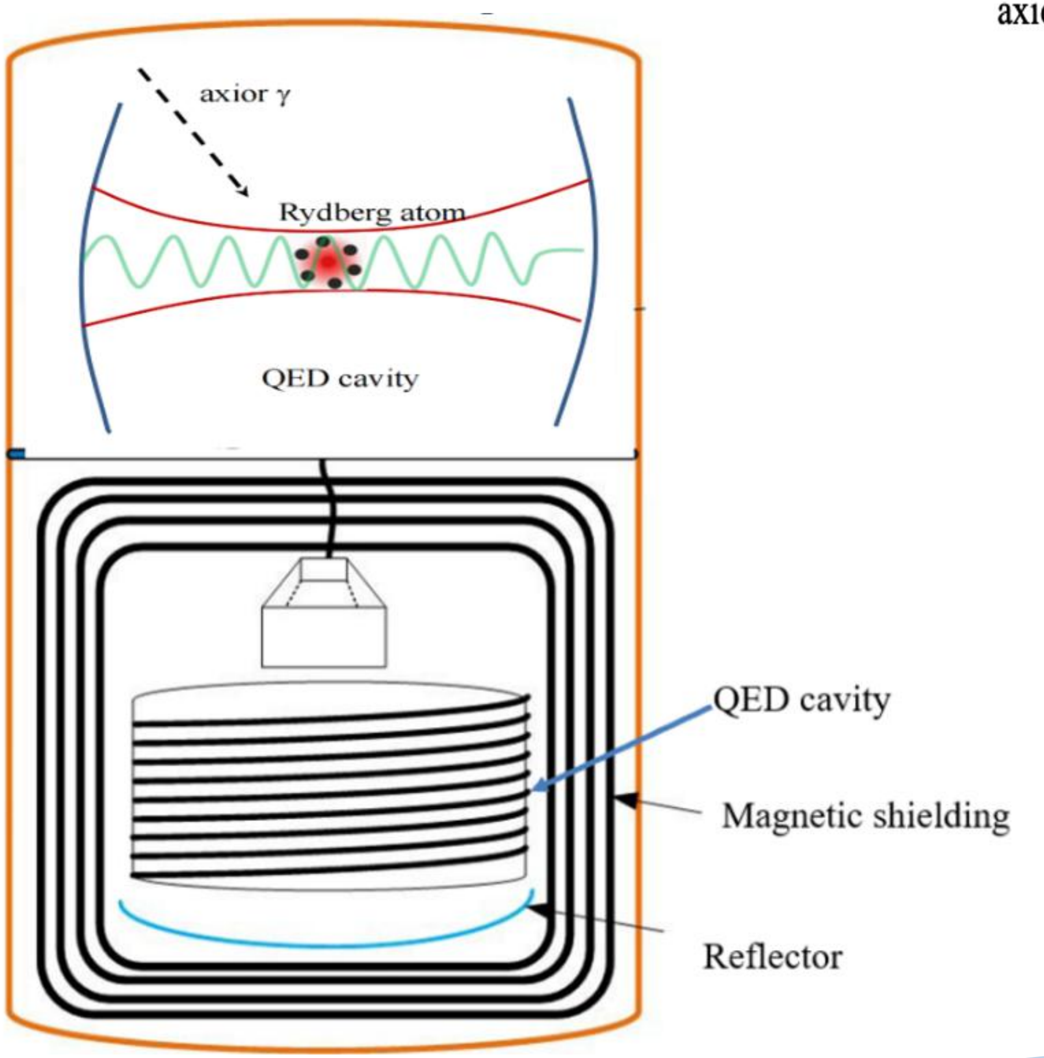

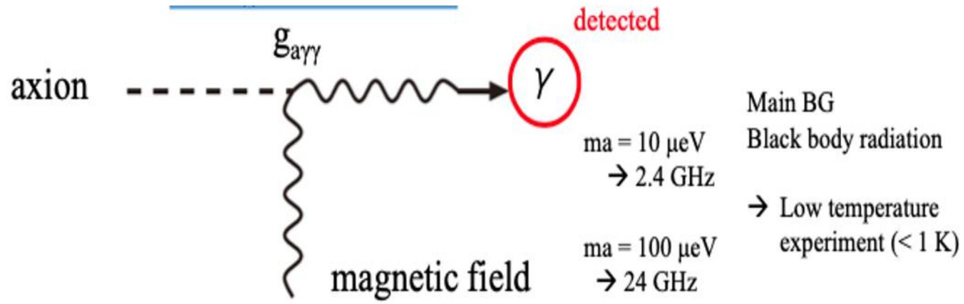

The microwave signal converted by the axion under the strong magnetic field is collected by the antenna horn, and the signal is led out by the waveguide to the Rydberg atomic gas chamber.

Low temperature: ~ 50mK

Main challenges:

- Reduce the noise from blackbody radiation: low temperature ~50 mK
- Keep atoms in gaseous state at 50mK temperature.

  Just like CARRACK: using the atom beam.

- Effectively capture the photon generated from the Axion.

  Another recent proposal by Engelhardt et al., (arxiv:2304.05863)

  Put the Rydberg atom in the strong magnetic field, axion-indued dipole transition.

Rydberg-based Axion search at Yale (RAY)

Detection Scheme

We are building a haloscope setup with Rydberg atom-based single photon detectors.

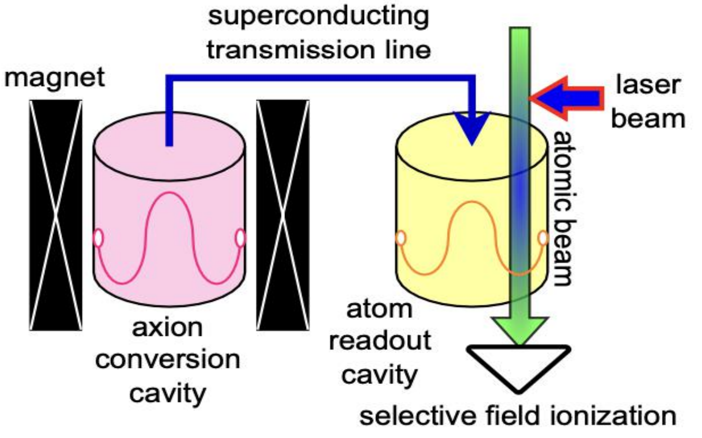

Above: A detection cavity is coupled to and locked in frequency with the conversion cavity.
Below: The system is cooled with a dilution refrigerator to reduce thermal noise.

Using ^{39}K Rydberg Atoms

Our setup will use ^{39}K, which is less susceptible to Stark shift than the Rb used by CARRACK [5]. Rydberg transitions in ^{39}K were found with electromagnetically induced transparency (EIT) spectroscopy [6].

Right: Laser wavelengths used for EIT on a ^{39}K energy level diagram. **Below:** EIT signal measured for the $n = 63$ Rydberg level [6], to which the Rydberg excitation lasers will be locked.

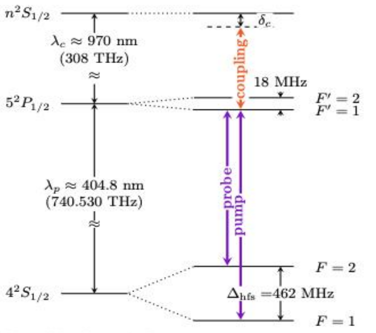

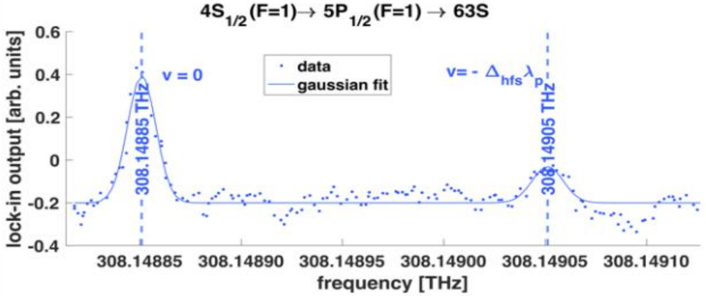

https://wlab.yale.edu/
https://maruyama-lab.yale.edu/

Funded by NSF award DMR-1747426 & the DOE-HEP QuantISED Program.

Below: Our EIT setup. The two blue diode lasers are frequency-locked using spectroscopy, so that the ^{39}K atoms can be raised to the Rydberg state with a two-photon transition using a photon from each laser.

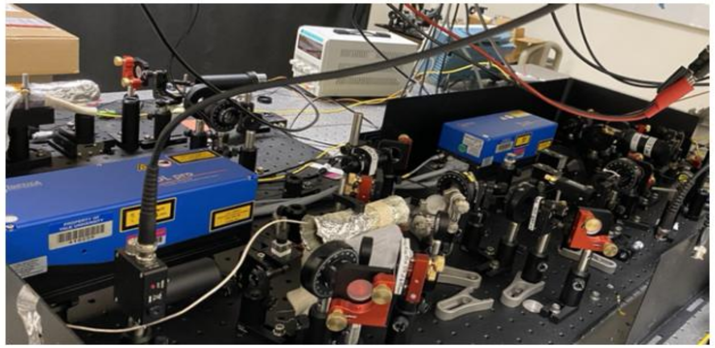

References:

[1] S. K. Lamoreaux, K. A. van Bibber, et al., "Analysis of single-photon and linear amplifier detectors for microwave cavity dark matter axion searches", Phys. Rev. D **88**, 035020 (2013).

[2] K. Backes, D. Palken, et al., "A quantum enhanced search for dark matter axions", Nature **590**, 238–242 (2021).

[3] A. V. Dixit, S. Chakram, et al., "Searching for dark matter with a superconducting qubit", Phys. Rev. Lett. **126**, 141302 (2021).

[4] C. O'HARE, *Cajohare/axionlimits: axionlimits*, version v1.0, July 2020.

[5] M. Tada, Y. Kishimoto, et al., "CARRACK II—a new large-scale experiment to search for axions with Rydberg-atom cavity detector", Nuclear Physics B-Proceedings Supplements **72**, 164–168 (1999).

[6] Y. Zhu, S. Ghosh, et al., "EIT spectroscopy of high-lying Rydberg states in ^{39}K", Phys. Rev. A **105**, 042808 (2022).

Research progress

- The multi-channel quantum receiving antenna
- Laser control circuit
- Frequency power stabilization control circuit
- Signal acquisition circuit
- Miniaturized integrated optical detector
- Multichannel signal real-time processing software system

Completed:

- Microwave target recognition
- Microwave frequency identification
- Functional verification of near-field antenna test

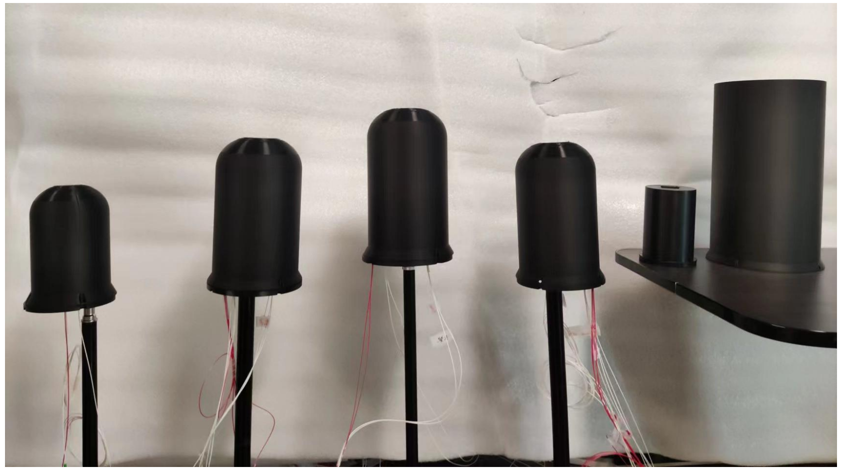

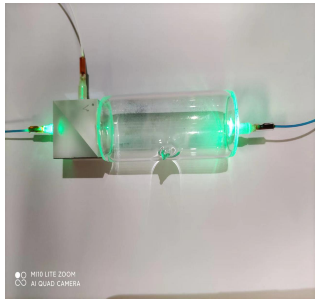

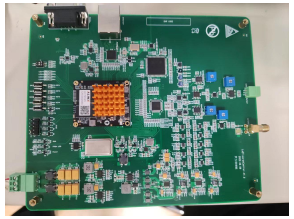

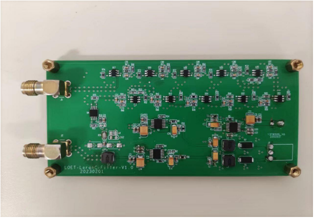

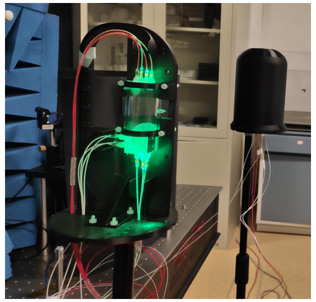

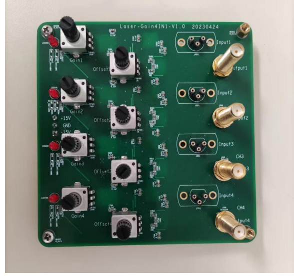

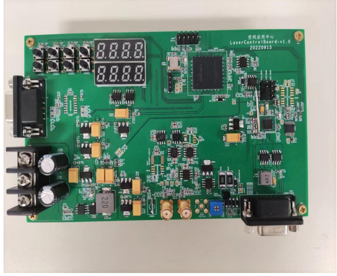

Research progress: from our collaborator

中国科学院空间应用工程与技术中心

Technology and Engineering Center for Space Utilization, Chinese Academy of Sciences

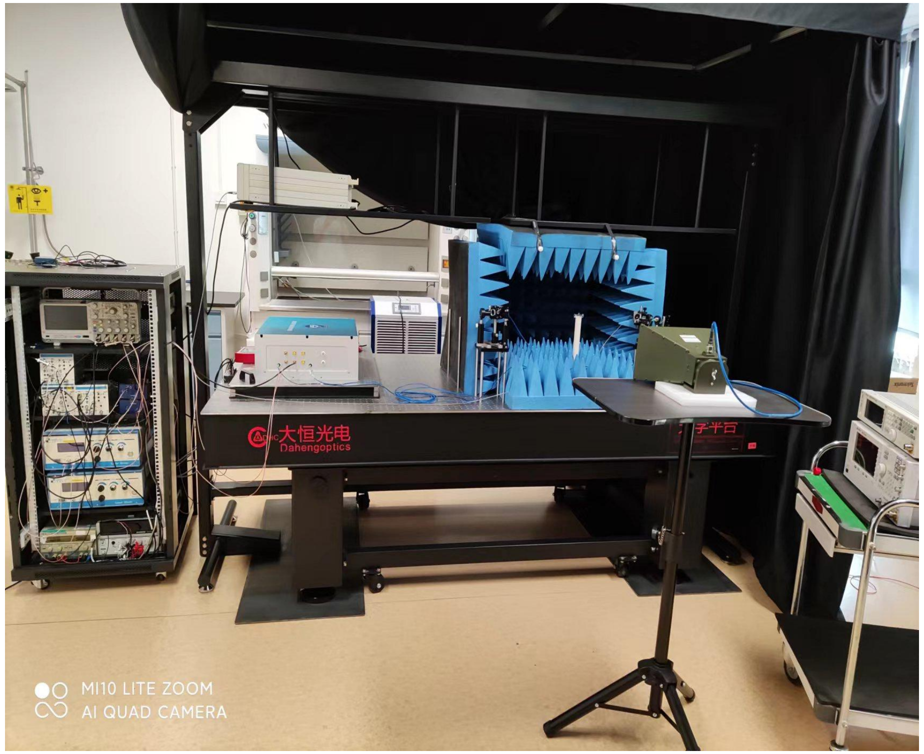

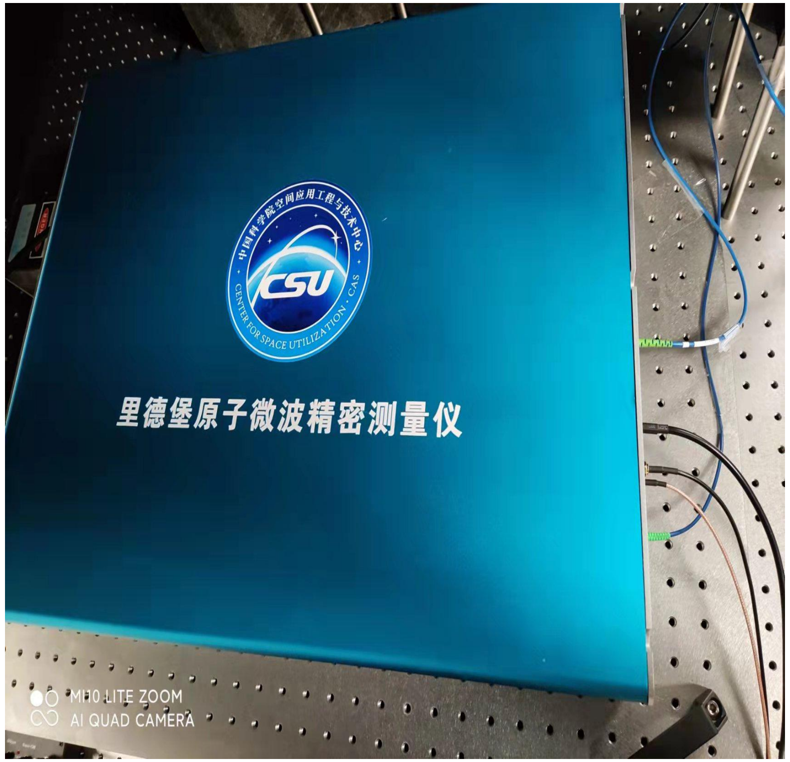

Miniaturized optical integration

Miniaturized all-optical probe

Progress In Sichuan University

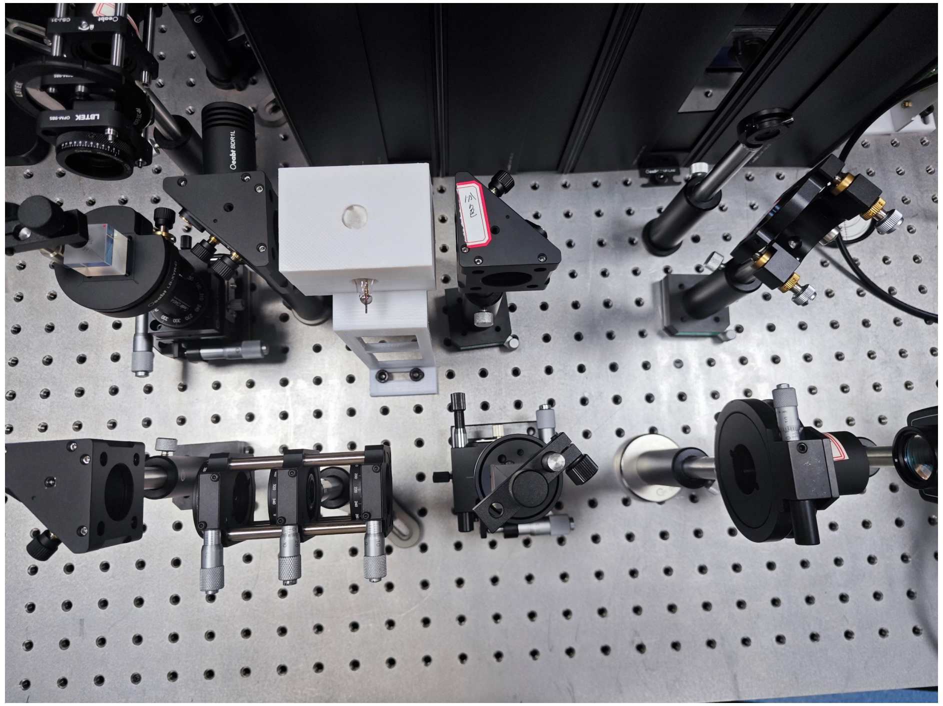

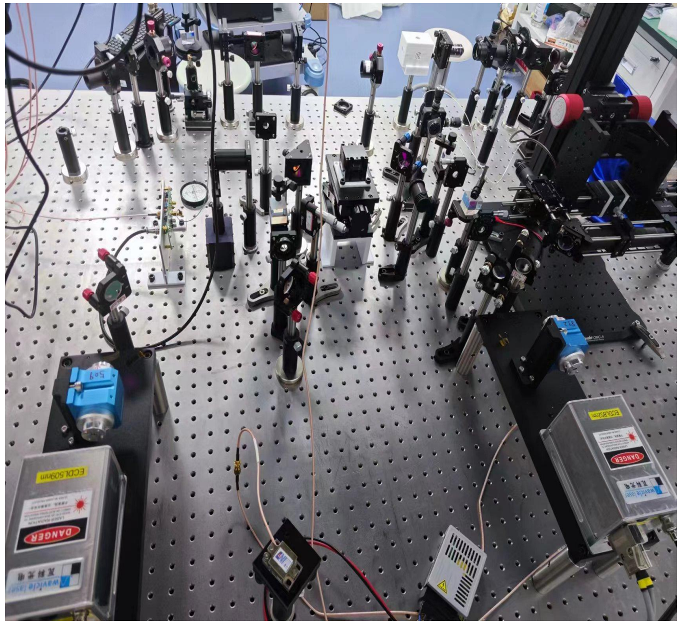

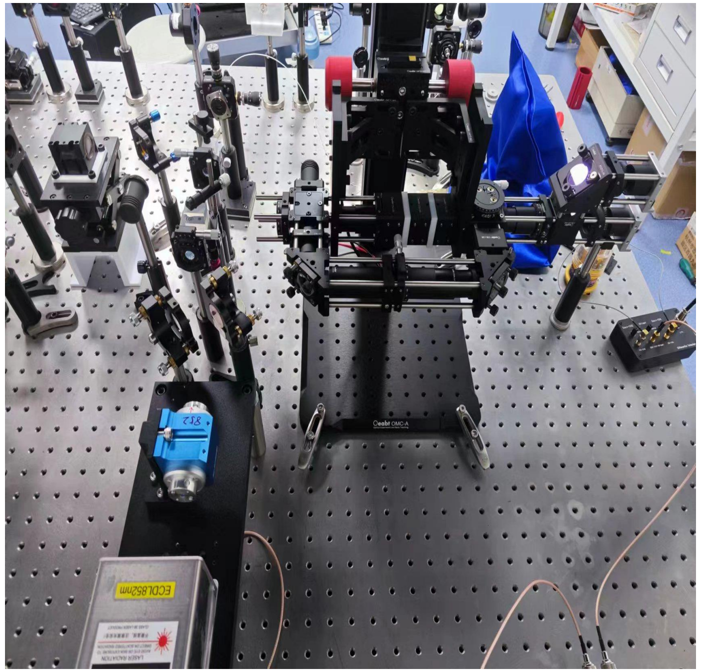

Optical Platform

Summary:

- Cavity haloscope is not suitable for detection of axion with higher mass >50uev

- Using Rydberg atom in detection of the microwave generated by Axion is promising in this energy region.

- It is in its infancy stage, many challenges, opportunities.

Thank you !